Anomalous strain effect in heteroepitaxial $SrRuO_3$ films on (111) $SrTiO_3$ substrates

Zhenzhen Wang(王珍珍)[1,2], Weiheng Qi(戚炜恒)[2,3], Jiachang Bi(毕佳畅)[4], Xinyan Li(李欣岩)[1], Yu Chen(陈雨)[3], Fang Yang(杨芳)[1], Yanwei Cao(曹彦伟)[4], Lin Gu(谷林)[5], Qinghua Zhang(张庆华)[1], Huanhua Wang(王焕华)[3], Jiandi Zhang(张坚地)[1], Jiandong Guo(郭建东)[1,2,6,†], and Xiaoran Liu(刘笑然)[1,‡]

[1] *Beijing National Laboratory for Condensed Matter Physics and Institute of Physics, Chinese Academy of Sciences, Beijing* 100190, *China*
[2] *School of Physical Sciences, University of Chinese Academy of Sciences, Beijing* 100049, *China*
[3] *Institute of High Energy Physics, Chinese Academy of Sciences, Beijing* 100049, *China*
[4] *Ningbo Institute of Materials Technology and Engineering, Chinese Academy of Sciences, Ningbo* 315201, *China*
[5] *Beijing National Center for Electron Microscopy and Laboratory of Advanced Materials, Department of Materials Science and Engineering, Tsinghua University, Beijing* 100084, *China*
[6] *Songshan Lake Materials Laboratory, Dongguan* 523808, *China*

(Received 4 May 2022; revised manuscript received 19 June 2022; accepted manuscript online 5 August 2022)

We report comprehensive investigations into the structure of high-quality (111)-oriented $SrRuO_3$ films on $SrTiO_3$ substrates to elucidate the effect of (111) heteroepitaxial strain. We found that $SrRuO_3$ film with a thickness of ~ 40 nm is compressively strained in plane on the substrate with full coherency. Nevertheless, the out-of-plane spacing is almost the same as in the bulk, which is at odds with the conventional paradigm. By probing a series of half-order Bragg reflections using synchrotron-based x-ray diffraction combined with analyses of the scanning transmission electron microscopy images, we discovered that the heteroepitaxial strain is accommodated via significant suppression of the degree of c^+ octahedral tilting and the formation of three equivalent domain structures on the (111) $SrTiO_3$ substrate. This anomalous effect sheds light on the understanding of an unconventional paradigm of film–substrate coupling for the (111) heteroepitaxial strain.

Keywords: perovskite $SrRuO_3$, (111)-oriented thin films, heteroepitaxial strain, octahedral tilt and rotation

PACS: 68.55.–a, 77.80.bn, 81.15.–z **DOI:** 10.1088/1674-1056/ac8725

1. Introduction

Heteroepitaxy is a powerful avenue for exploring and tailoring novel properties of transition metal oxides with synergistic couplings of various degrees of freedom.[1–5] The asymmetries in lattice, charge, orbital and spin degrees of freedom at the interface between the film and substrate lead to the emergence of latent or hidden phenomena that are inaccessible in bulk materials.[1,6] Heteroepitaxial engineering has been widely utilized in the material families of perovskite oxides (chemical formula ABO_3) whose structure is characteristic of the three-dimensional network of corner-sharing BO_6 octahedra. While the ideal symmetry of ABO_3 is cubic, adjacent BO_6 octahedra can rotate and the overall symmetry is lowered as a result of the mismatches between A and B cations, which is determined by the so-called 'tolerance factor'.[7,8]

Scenarios of coupling between perovskite oxide thin films and substrates have been extensively explored for (001)-oriented epitaxy.[9–15] In this situation, since those two orthogonal directions of (001) biaxial strain coincide with the principal axes of the pseudo-cubic unit cell, it has been generally rationalized that the effect of a compressive (tensile) strain would increase (decrease) the out-of-plane lattice parameter, and further enhance (suppress) the octahedral rotations around the out-of-plane axis.[15–20] However, with recent advances in the fabrication of high-quality perovskite oxide epitaxial films along other crystallographic orientations, much less knowledge about the strain effect has been revealed thus far compared with the (001) case. Especially for the case of (111) heteroepitaxy, none of the three tilting axes are parallel or perpendicular to the strain plane, such that the paradigm described above for (001) strain is no longer applicable. Whether or not the epitaxial strain is still preserved, and how it would affect the physical properties of films, remains unclear.[21–24]

In this work, to address these issues we focus on the 4d transition metal oxide $SrRuO_3$ (SRO). As one of the most representative perovskite oxides, heteroepitaxial thin films of (001)-oriented SRO have attracted tremendous research interest for decades.[25] The conventional unit cell of bulk SRO is illustrated in Fig. 1(a). SRO possesses an orthorhombic *Pbnm* crystal structure with the lattice parameters $a = 5.5670$ Å, $b = 5.5304$ Å, and $c = 7.8446$ Å.[25] The RuO_6 octahedra rotate in the same manner (in-phase) along the pseudo-cubic $[010]_{PC}$ and $[001]_{PC}$ directions, and in the opposite manner (anti-phase) along the pseudo-cubic $[100]_{PC}$ direction, leading to an '$a^-a^-c^+$' tilting pattern in Glazer notation[26] and a

†Corresponding author. E-mail: jdguo@iphy.ac.cn
‡Corresponding author. E-mail: xiaoran.liu@iphy.ac.cn

© 2022 Chinese Physical Society and IOP Publishing Ltd

pseudo-cubic lattice constant of ∼ 3.93 Å. High-quality SRO epitaxial thin films have been fabricated on [111]-oriented $SrTiO_3$ (STO) substrates. X-ray diffraction (XRD) and reciprocal space mapping (RSM) data demonstrate that the SRO thin film is compressively strained on the substrate with complete coherency. Nevertheless, it is surprising that the out-of-plane lattice parameter is rarely varied, at odds with the conventional paradigm. Scanning transmission electron microscopy (STEM) images confirm the coherency and sharpness of the film–substrate interface and shed light on the suppression of the c^+ tilting inside the film. Synchrotron-based XRD on a series of half-ordering reflections clearly demonstrates the establishment of three equivalent domain structures of SRO on the (111)-oriented STO substrate, each of which hosts the $a^-a^-c^+$ tilting pattern with significant suppression of the c^+ tilting angle compared with bulk SRO. These experimental findings highlight a peculiar paradigm for the accommodation of (111) strain, and pave a new route towards turning the properties of oxide thin films via strain engineering along other crystallographic directions.

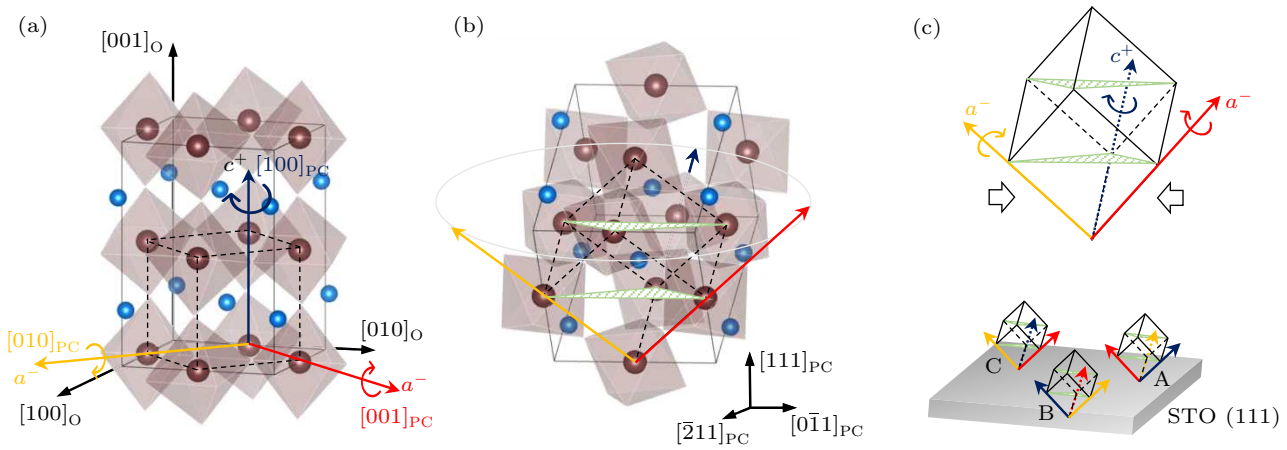


Fig. 1. (a) Schematic illustration of the orthorhombic (O) conventional unit cell and the pseudo-cubic (PC) unit cell of SRO. The three axes of RuO_6 tilting are along the pseudocubic ⟨100⟩ directions. (b) Transformation of the structure in the case of a $(111)_{PC}$ epitaxial relationship. The (111) planes are highlighted using shadowed green lines. (c) SRO under (111) compressive strain. Three equivalent domain structures (A, B, and C) can be epitaxially stabilized on the STO (111) surface.

2. Methods

The general relationship between (001)- and (111)-oriented epitaxial SRO thin films is illustrated in Figs. 1(a) and 1(b). High-quality SRO thin films were fabricated on STO (111) substrates by means of pulsed laser deposition equipped with reflection high-energy electron diffraction. The films were deposited at a substrate temperature of ∼ 730 °C under an oxygen partial pressure of ∼ 10 Pa. A ceramic SRO target with the proper chemical stoichiometry was ablated by a KrF excimer laser at a pulse frequency of 2 Hz ($\lambda = 248$ nm, laser fluence ∼ 2 J·cm^{-2}). After deposition, the films were annealed at the growth condition for 10 min and cooled down to room temperature. XRD and RSM data were recorded using a Rigaku SmartLab diffractometer. All the indices mentioned in this work are defined in cubic (or pseudo-cubic) notation unless otherwise stated. High-resolution cross-sectional STEM images were taken in the high-angle annular dark-field (HAADF) mode. The sample was cut and projected on the $(11\bar{2})_{PC}$ plane. Synchrotron-based XRD experiments were performed at beamline 1W1A of the Beijing Synchrotron Radiation Facility. The photon energy was fixed at 8.05 keV during the measurements. Alignment and scans were recorded using the reciprocal lattice unit (r.l.u.) of the STO substrate.

3. Results and discussion

The XRD 2θ–ω symmetric scans along the {111} planes of SRO film exhibit sharp (222) peaks on the left side of the STO (222) reflection, as shown in Fig. 2(a). The calculated spacing of the {111} planes is $d_{111} \sim 2.27$ Å, practically the same as that of bulk SRO.[27] The film thickness is ∼ 40 nm, as demonstrated from the x-ray reflectivity scans with fitting (Fig. 2(b)), which is consistent with the counting of the pulse numbers during the deposition. Figure 2(c) shows the RSM scans around the STO (312) reflection in an attempt to reveal the in-plane lattice constant and status of the strain of films. As indicated by the black vertical line, it is surprising that the ∼ 40 nm thick SRO film still has the same in-plane component Q_x as the STO substrate, corroborating that the SRO film is fully strained to the substrate. The measured Q_z value of the SRO film is ∼ 8.78 nm^{-1}, corresponding to an out-of-plane spacing of ∼ 2.27 Å, in good agreement with the value extracted from XRD symmetric scans. These data immediately challenge the conventional picture of strain accommodation, where a compressive strain would stretch the out-of-plane lattice spacing. The combined results of XRD and RSM suggest an anomalous heteroepitaxial strain effect in 40 nm thick SRO on a STO (111) substrate.

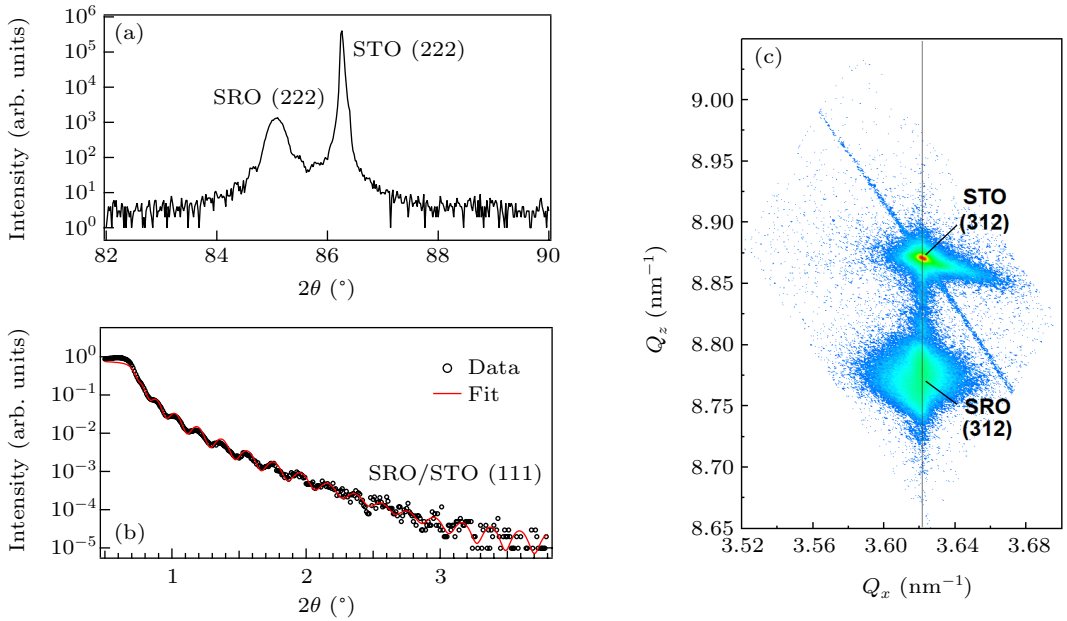


Fig. 2. (a) XRD 2θ–ω scans and (b) x-ray reflectivity (XRR) of SRO film grown on a STO (111) substrate. The thickness of the SRO/STO (111) film is $\sim$40 nm according to the XRR fitting. (c) Reciprocal space mapping scans near the STO (312) reflection.

To further characterize the tilting pattern of RuO_6 octahedra and to obtain real-space microscopic information about the film structure, we performed atomic-resolution aberration-corrected STEM imaging on the (111) SRO sample. Figure 3(a) shows the HAADF-STEM image obtained with the electron beams incident along the $[11\bar{2}]$ direction, which clearly demonstrates the high quality and uniformity of our SRO film with full coherency. Note that only the Sr, Ru and Ti atoms are visible in the HAADF mode as the intensity of atoms is proportional to Z^2 (Z being the atomic number). In order to reach an accurate estimation about the positions of atoms, the STEM image was replotted using CalAtom software.[28] Figure 3(b) shows a representative image of the resultant mapping on a zoomed area as outlined by the red rectangle in Fig. 3(a). The corresponding schematic structure of bulk SRO (space group *Pbnm*) is displayed in Fig. 3(c) projected along the $[11\bar{2}]$ direction, which is consistent with the STEM images. The right pattern of Fig. 3(c) shows the ideal tilt of the Sr sublattice along the [111] direction in bulk SRO, indicating that the structural characteristics of orthorhombic SRO possessing the $a^-a^-c^+$ rotation pattern can be ascribed to the tilting of the Sr sublattice. Accordingly, the c^+ octahedral tilt is indicated as the relative Sr–Sr displacement (δ_{Sr}), as depicted in Fig. 3(b). We carried out quantitative analyses on δ_{Sr} by extracting their values from the HAADF images along the [111] direction, as shown in Fig. 3(d). Note that the data for each unit cell were obtained by statistically averaging over 10 adjacent rows. The δ_{Sr} on the substrate side is practically zero, which agrees well with the cubic symmetry of STO (i.e., no tilt). On the side of the SRO film, the expected value of δ_{Sr} in its bulk due to c^+ octahedral tilt is marked by two dotted lines. As seen, while there is a finite magnitude of tilt in the Sr sublattice, it is much smaller than the theoretical value. These analyses provide strong evidence for the significant suppression of c^+ rotation in our SRO film under compressive (111) strain.

More comprehensive investigations about the tilting pattern of RuO_6 octahedra in our (111) compressively strained SRO thin films were carried out by probing a series of half-order Bragg reflections using synchrotron-based XRD. Specifically, for SRO with the $a^-a^-c^+$ tilting pattern, {odd/2 odd/2 odd/2}-type reflections (odd refers to an odd integer) with $k \neq l$ ($h \neq l$) are produced due to anti-phase tilting around the a (b) rotation axis; whereas {odd/2 odd/2 even/2}-type reflections (even refers to an even integer) with $h \neq k$ are produced due to in-phase tilting around the c-axis.[26] This is indeed demonstrated through the observations of the (1/2 3/2 1/2), (3/2 1/2 1/2), and (1/2 3/2 1) reflections, as shown in Fig. 4. However, it is striking that other reflections with indices of {even/2 odd/2 odd/2} and {odd/2 even/2 odd/2}, for example the (1 1/2 3/2) and (3/2 1 1/2) peaks, are also present, indicating the existence of in-phase tilting around the a and b rotation axes as well. In particular, it is noteworthy that the intensities of these peaks, which are in principle proportional to the square of the corresponding tilting angles, are practically the same for the three half-order reflections containing one even index. Similarly, those three 'odd–odd–odd' style half-order peaks also exhibit a very close magnitude of intensities. These phenomena are plausibly interpreted as a result of hexagonal symmetry of the STO (111)

surface, which triggers the formation of three equivalent domain structures in the SRO epitaxial thin films, depending on the specific selection of the in-phase tilting axis out of the three ⟨100⟩ directions.

Another point worth noting is that, based on the relationships between the intensities of the half-order reflections and the tilting angles in the $a^-a^-c^+$ tilting pattern, $I(c^+) \propto (hi^k - ki^h)\gamma^2$; $I(a^-) \propto \left((ki^l - li^k)\alpha + (hi^l - li^h)\alpha + (hi^k - ki^h)\gamma\right)^2$.[26] As a result, the intensity of (1/2 3/2 1) is proportional to γ^2 while the intensity of (1/2 3/2 1/2) is proportional to $(\alpha - \gamma)^2$. For bulk SRO with an anti-phase tilting angle $\alpha \sim 9.9°$ and an in-phase tilting angle $\gamma \sim 10.2°$, the intensity of (1/2 3/2 1) is expected about three orders of magnitude higher than that of (1/2 3/2 1/2). However, as seen in Fig. 4, the intensity of (1/2 3/2 1) is even lower than that of (1/2 3/2 1/2) for the SRO thin film on the (111) STO substrate, indicating that the degree of the in-phase tilting angle is significantly suppressed. These results reveal an intriguing paradigm that the effect of biaxial strain in the (111) plane is accommodated via the modification of a peculiar octahedral tilting, rather than the conventional way of stretching or compressing the out-of-plane spacing as typically seen in the (001) situation.

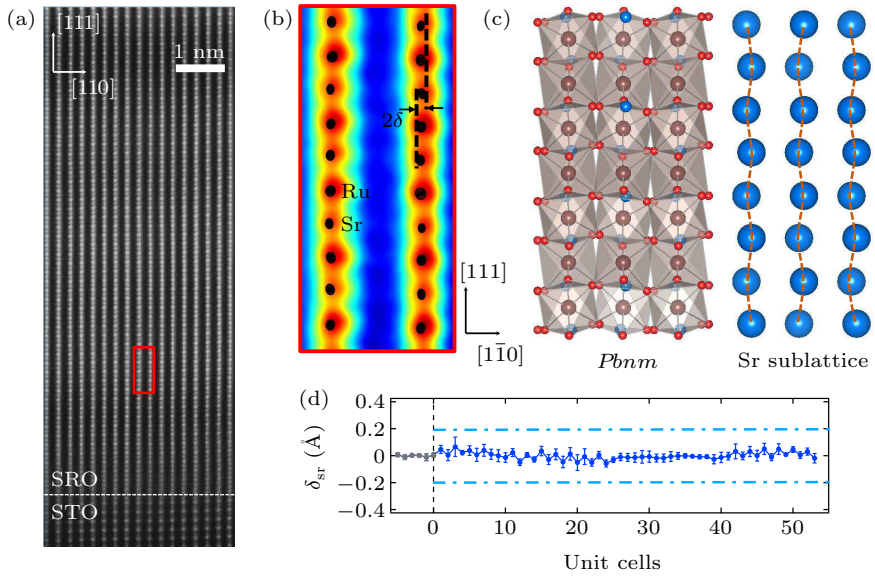


Fig. 3. (a) High-resolution high-angle annular dark-field scanning transmission electron microscopy (HAADF-STEM) image of SRO film. The HAADF-STEM images were obtained along the [11$\bar{2}$] zone axis. (b) An example of the replotted STEM image using CalAtom software. (c) Schematic diagrams of orthorhombic bulk SRO (space group *Pbnm*). The tilt of the individual Sr sublattice is shown on the right of (c). (d) The plot of experimentally measured δ_{Sr} from the substrate to the surface of the SRO film. The error bars represent standard deviation.

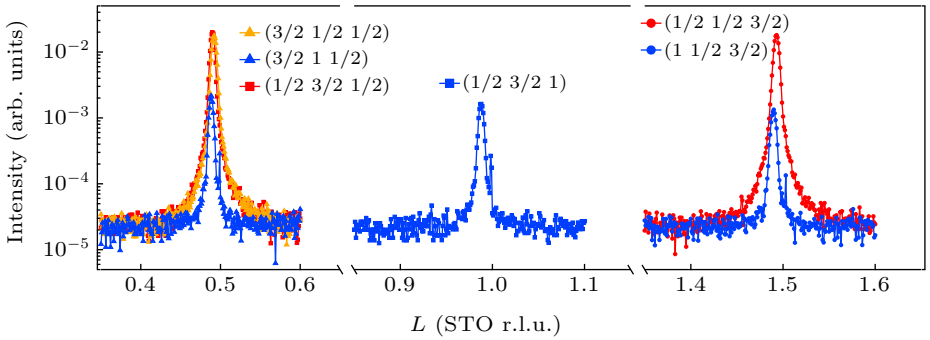


Fig. 4. Synchrotron-based XRD HKL-coupled scans on a series of half-ordering reflections of the SRO epitaxial film grown on (111) STO substrate. The measurements were taken at 300 K with an incident photon energy of 8.05 keV (λ = 1.5438 Å). Data are plotted in STO r.l.u. such that the peaks of the film deviate slightly from the exact half-ordering indices.

4. Conclusion

In summary, we have investigated the effect of (111) heteroepitaxial strain on high-quality SRO thin films on STO (111) substrates. We discovered an anomalous scenario of film–substrate coupling, where the compressive strain is accommodated not via stretching of the out-of-plane lattice spacing as expected in the conventional scenario but via the significant suppression of the degree of a peculiar octahedral rotation. These findings can potentially open new avenues for changing the physical properties of films via strain engineering.

Acknowledgments

Project supported by the National Key Research and Development Program of China (Grant No. 2017YFA0303600), the National Natural Science Foundation of China (Grant No. 11974409), and the Strategic Priority Research Program (B) of the Chinese Academy of Sciences (Grant No. XDB33000000).

References

[1] Hwang H Y, Iwasa Y, Kawasaki M, Keimer B, Nagaosa N and Tokura Y 2012 *Nat. Mater.* **11** 103
[2] Chakhalian J, Freeland J W, Millis A J, Panagopoulos C and Rondinelli J M 2014 *Rev. Mod. Phys.* **86** 1189
[3] Ohtomo A and Hwang H Y 2004 *Nature* **427** 423
[4] Li D, Lee K, Wang B Y, Osada M, Crossley S, Lee H R, Cui Y, Hikita Y and Hwang H Y 2019 *Nature* **572** 624
[5] Bhattacharya A, May S J, Te Velthuis S G E, Warusawithana M, Zhai X, Jiang B, Zuo J M, Fitzsimmons M R, Bader S D and Eckstein J N 2008 *Phys. Rev. Lett.* **100** 257203
[6] Huang Z, Ariando, Renshaw Wang X, Rusydi A, Chen J, Yang H and Venkatesan T 2018 *Adv. Mater.* **30** 1802439
[7] Peña M A and Fierro J L G 2001 *Chem. Rev.* **101** 1981
[8] Dagotto E and Tokura Y 2008 *MRS Bulletin* **33** 1037
[9] Yoon S, Gao X, Ok J M, Liao Z, Han M G, Zhu Y, Ganesh P, Chisholm M F, Choi W S and Lee H N 2021 *Nano Lett.* **21** 4006
[10] Vailionis A, Boschker H, Siemons W, Houwman E P, Blank D H A, Rijnders G and Koster G 2011 *Phys. Rev. B* **83** 064101
[11] Liao Z, Huijben M, Zhong Z, Gauquelin N, Macke S, Green R J, Van Aert S, Verbeeck J, Van Tendeloo G, Held K, Sawatzky G A, Koster G and Rijnders G 2016 *Nat. Mater.* **15** 425
[12] Kan D, Aso R, Sato R, Haruta M, Kurata H and Shimakawa Y 2016 *Nat. Mater.* **15** 432
[13] Aso R, Kan D, Shimakawa Y and Kurata H 2013 *Sci. Rep.* **3** 2214
[14] Aso R, Kan D, Shimakawa Y and Kurata H 2014 *Adv. Funct. Mater.* **24** 5177
[15] Adamo C, Ke X, Wang H Q, Xin H L, Heeg T, Hawley M E, Zander W, Schubert J, Schiffer P, Muller D A, Maritato L and Schlom D G 2009 *Appl. Phys. Lett.* **95** 112504
[16] Moreau M, Marthinsen A, Selbach S M and Tybell T 2017 *Phys. Rev. B* **95** 064109
[17] Rondinelli J, May S and Freeland J 2012 *MRS Bulletin* **37** 261
[18] Aruta C, Ghiringhelli G, Tebano A, Boggio N G, Brookes N B, Medaglia P G and Balestrino G 2006 *Phys. Rev. B* **73** 235121
[19] He J, Borisevich A, Kalinin S V, Pennycook S J and Pantelides S T 2010 *Phys. Rev. Lett.* **105** 227203
[20] Kinyanjui M K, Lu Y, Gauquelin N, Wu M, Frano A, Wochner P, Reehuis M, Christiani G, Logvenov G, Habermeier H U, Botton G A, Kaiser U, Keimer B and Benckiser E 2014 *Appl. Phys. Lett.* **104** 221909
[21] Chakhalian J, Liu X and Fiete G A 2020 *APL Mater.* **8** 050904
[22] Wang Y, Liang Y, Meng M, An Q, Ge B, Liu M, Yang F and Guo J 2020 *J. Appl. Phys.* **128** 035301
[23] Saghayezhian M, Wang Z, Guo H, Zhu Y, Plummer E W and Zhang J 2017 *Phys. Rev. B* **95** 165434
[24] Kim T H, Puggioni D, Yuan Y, Xie L, Zhou H, Campbell N, Ryan P J, Choi Y, Kim J W, Patzner J R, Ryu S, Podkaminer J P, Irwin J, Ma Y, Fennie C J, Rzchowski M S, Pan X Q, Gopalan V, Rondinelli J M and Eom C B 2016 *Nature* **533** 68
[25] Koster G, Klein L, Siemons W, Rijnders G, Dodge J S, Eom C-B, Blank D H A and Beasley M R 2012 *Rev. Mod. Phys.* **84** 253
[26] Glazer A M 1975 *Acta Cryst.* **A31** 756
[27] Lee B, Kwon O U, Shin R H, Jo W and Jung C U 2014 *Nanoscale Research Letters* **9** 8
[28] Zhang Q, Jin C H, Xu H T, Zhang L Y, Ren X B, Ouyang Y, Wang X J, Yue X J and Lin F 2018 *Micron* **113** 99